Geometric and Electronic Structures of Vanadium Sub-nano Clusters, V_n (n = 2-5), and their Adsorption Complexes with CO and O_2 Ligands: A DFT-NBO Study

A.H. Pakiari* and F. Eshghi

Department of Chemistry, College of Science, Shiraz University, Eram Square, Eram Street, 7146713565, Shiraz, Iran

(Received 18 March 2017, Accepted 28 May 2017)

In this study, electronic structures of ground state of pure vanadium sub-nano clusters, V_n (n = 2-5), and their interactions with small ligands, CO and triplet O_2 molecules, are investigated using density functional theory (DFT) calibration at the mPWPW91/QZVP level of theory. The favorable orientations of these ligands in interaction with pure vanadium sub-nano clusters were determined. Multiplicities of these pure clusters are triple, doublet, singlet and doublet for dimer, trimer, tetramer and pentamer, respectively. While the CO molecule is associatively adsorbed on vanadium clusters, triplet O_2 is dissociated over adsorption. Primary and secondary hyper-conjugation concepts have been employed to show stabilization of vanadium oxide complexes. Natural bond orbital (NBO) and natural resonance theory (NRT) analyses revealed that trimer, tetramer and pentamer clusters are relatively delocalized and have some resonance structures.

Keywords: Transition metal clusters, Metal-metal multiple bond, Organometallic compounds, Catalytic activity

INTRODUCTION

About 90 years ago, the first publication concerning of synthesis of metal clusters was published [1]. Metal cluster means at least two metals directly are bonded [2]. Properties of metal clusters are affected by their size and composition [3,4]. One of the interesting aspects of metal clusters is that they somehow reproduce the behavior of metal surfaces despite some conspicuous and undeniable differences between these two entities. Among metal clusters, transition metal (TM) clusters have attracted significant attention due to their wide spread applications [5-15]. The TM clusters are largely used in organometallic compounds [10,16]. Our attention in this investigation is on small vanadium clusters. These types of organometallic compounds contain two to five and sometimes up to ten TM atoms [16] and have especal properties, such as drug [9] anticancer [10-12] catalysis [16], *etc*.

Vanadium is an early (hypovalent) TM element which its clusters have extensive applications in organometallic

---

*Corresponding author. E-mail: pakiariah@gmail.com

compounds such as $(arene)_2V_2$ and $Pn*_2V_2$ ($Pn*$ = C_8Me_6) [7,8]. Ozin and Andrews [7] mentioned that these complexes can be better formulated with having knowledge of electronic structure (type of bond, bond order, highest occupied molecular orbital (HOMO) and lowest unoccupied molecular orbital (LUMO) of vanadium clusters. Since sub-nano vanadium clusters are building block of some organometallic compounds [7,8], their structures and electronic properties of these small clusters are important.

Theoretical studies have been extensively carried out on pure vanadium clusters in past years [17-20]. Structure of vanadium clusters has been studied using density functional theory (DFT) by Grönbeck and Rosen, [18] and by Wu and Ray [19]. Adsorption of ligand on TM clusters has a profound effect on catalytic reactions [13] magnetization [21] and reactivity [22]. Reactivity of vanadium clusters with small molecules such as CO, O_2, N_2, CH_3OH and some organic molecules have been the subject of some recent studies [16,22-24]. Interaction of CO molecule with vanadium clusters can be used to predict the metal-CO bond strength in organometallic complexes, and mechanistic steps in the chemical reaction pathways [25,26]. Vanadium

oxides as catalysts are very important in industrial processes [27] which help reaction of SO_2 oxidation in the synthesis of the sulfuric acid [28], or reduction of NO_x by ammonia [29,30]. Despite the abundance of theoretical works on vanadium clusters, the nature of metal-metal and metal-ligand bonds in pure vanadium clusters and their interaction with small ligands have not been considered yet.

Our approach for electronic structure is quantum chemical calculation by DFT procedure which determines the types of bonds, occupation, hybridization, HOMO and LUMO, charge transfer and their possible resonances structures. These properties can be more understandable for chemists in language of orbital localization. Therefore, a powerful localization procedure named "natural bond orbital (NBO)" is used [31,32]. Theoretical calculations give a complete picture of geometric and electronic structures of clusters and their complexes with small ligands. Accordingly, at first, through a DFT-based study, we search for geometric structures of pure vanadium clusters, V_n ($n =$ 2-5). At the second stage, we try to identify the favorable adsorption sites of neutral ligands such as CO and triplet O_2 on vanadium clusters. Finally, we will investigate the nature of metal-metal and metal-ligand bonds in pure vanadium clusters and their complexes with small ligands, respectively.

COMPUTATIONAL METHODS

Geometric and electronic structure calculations were performed using Gaussian 09 program package [33] based on DFT methods, which is known as an appropriate tool to study the first row TM clusters [34-37]. DFT would provide an exact solution if we know *xc*-functional. Since the exact *xc*-functional is not known until now, the approximate one is always used, therefore, DFT is not variational. We search to find appropriate *xc*-functional and basis set for our case, this procedure is called calibration, which will be discussed with more details in results and discussion part. So, mPWPW91 *xc*-functional [38,39] within the generalized gradient approximation (GGA) [40] was chosen as a proper functional for vanadium cluster and their complexes. Gaussian basis set of quadruple zeta valence polarize (QZVP) [41] quality was chosen also for these calculations. Frequency calculations were performed

for all species to ensure that all the optimized geometries have no imaginary frequencies.

Assignment of the ground spin state (definite multiplicity) is another point which has been always a controversial aspect of TM clusters, even for the smallest ones. This difficulty is due to the nearly degenerate energy levels of TMs, which make the identification of ground state very difficult. Accordingly, for each cluster, optimization is performed for possible spin multiplicities until the lowest spin contamination (accuracy 10^{-2}) is reached. This guarantees having pure spin state wave function.

The bond dissociation energy (BDE) and adiabatic ionization potential (IP_{ad}) are used in DFT calibration section. The BDE is defined as the required energy to fragmentize the V_n cluster into V_{n-1} and V atoms. The BDE and IP_{ad} of clusters are evaluated by $E_{BDE} = (E_{V_{atom}} + E_{V_{n-1}}) - E_{V_n}$ and $IP_{ad} = E_{V_n}^+ - E_{V_n}$ equations, respectively. Neutral (V_n clusters and V atom) and charged (cationic clusters) species are in the lowest energy structures. In complexes, binding (adsorption) energy, interaction energy, and Gibbs free energy were calculated. The thermodynamic stability of the system is described by binding energy:

$$E_{bind} = E_{complex} - (E_{cluster} + E_{ligand}) \qquad (1)$$

where $E_{complex}$ is the total energy of complex, $E_{cluster}$ and E_{ligand} are total energies of cluster and ligand. Due to the deformation of the species, this equation does not describe the quality of interaction well. So, interaction energy, E_{int}, is calculated as a function of bond strength [42-44] by Eq. (2):

$$E_{int} = E_{bind} - (\Delta E_{cluster} + \Delta E_{ligand}) \qquad (2)$$

where $E_{cluster}$ and ΔE_{ligand} are the deformation energies of metal cluster and lignad, respectively. Deformation energy is calculated as the difference between the energy of the free molecule in the gas phase geometry and the energy of the isolated and distorted molecule in its complex. The more negative values of E_{int} and E_{bind} indicate the more stable adsorption.The change of Gibbs free energy, ΔG, occurs when a complex is formed from cluster and ligand in their most thermodynamically stable states, Eq. (3):

$$\Delta G = \Sigma \Delta G_{complex} - \Sigma(\Delta G_{cluster} + \Delta G_{ligand}) \qquad (3)$$

where $\Delta G_{complex}$, $\Delta G_{cluster}$ and ΔG_{ligand} are free energies of the complex, cluster, and ligand, respectively.

The information about selected geometries of V_n ($n = 2$-5) clusters and V_nL complexes (L: CO and O_2 molecules) are completed by the results of the NBO analysis. NBO gives the information of type of the bond, bond order, HOMO and LUMO, occupancies, depletion of occupancies, percent of localization or delocalization (Lewis and non-Lewis) and stabilization energies (E^2_{ij}) [31,32]:

$$E^2_{ij} = \frac{\left|\left\langle i|\hat{H}|j\right\rangle\right|^2}{E_j - E_i} \qquad (4)$$

where $\hat{H}$ is interaction Hamiltonian, E_j and E_i are orbital energies, and $\left\langle i|\hat{H}|j\right\rangle$ is the matrix element.

RESULT AND DISCUSSIONS

In this part, you will see the results of calibration in Tables 1 and 2, the results of geometry optimization of vanadium clusters, BDE, IP, EA and bond length in Table 4, and the results of NBO containing NBO bonds, percentage of metal-metal hybridization, energy, and shape of bonding orbitals in α-and β-spin parts in dimer in Table 3 as a sample. Other clusters are presented in supplementary file as Tables 1s, 3s and 4s for trimer, tetramer and pentamer vanadium cluster, respectively. The results of vanadium clusters with CO and O_2 are presented in Tables 5 and 6. The primary and secondary hyper-conjugations for charge transfer in the V_nO_2 ($n = 2$-5) complexes are shown in Table 7. The remaining figures include the resonance structures of V_3 and V_4 clusters.

DFT Calibration for Vanadium Clusters

Despite its widespread applications of DFT [34-36], DFT-based calculations strongly depend on the *xc*-functionals and basis sets. In other words, different *xc*-functionals have different predictions of TM properties. Therefore, we calibrate different *xc*-functionals recommended for vanadium clusters with different basis sets in order to find the best results according to the correct

multiplicity (where experimental multiplicities were available) with 10^{-2} deviation, positive frequency and experimental geometry. In calibration process, we have compared our results with some reported experimental values for vanadium dimer: (spin multiplicity is triplet, bond length is 1.774 Å, vibrational frequency is 634.6 cm^{-1}, BDE is 2.74 eV, and IP$_{ad}$ is 6.64 eV [4,17,45,46]). Table 1 shows that the appropriate *xc*-functional and basis set would be mPWPW91/QZVP. Further support for our choice of this *xc*-functional and basis set is provided by calculating BDE and IP$_{ad}$ for vanadium clusters containing more atoms, V_n ($n = 3$-5). The results presented in Table 2 confirm that we can rely on the mPWPW91/QZVP level of theory to provide reliable results.

Geometric and Electronic Results

V_2 Cluster. The results of V_2 are considerably discussed in calibration (calibration section). Our calculated bond length and vibrational frequency are 1.774 Å and 634.6 cm^{-1}, respectively, which are in good agreement with Roos et al.'s results done by MCSCF [47], 1.77 Å and ν = 593.6 cm^{-1} for bond length and frequency, respectively. NBO analysis considers ten valence electrons for this small cluster; six electrons in α-spin (two non-degenerate sigma (σ), two degenerate pi (π), and two degenerate delta (δ) and four in β-spin part, (two non-degenerate σ and two degenerate π), and it does not have nonbonding (NB) orbital. The results are shown in Table 3. The β-spin part is more stable than the α-spin part, (15.31 kcal mol^{-1}). The HOMO belongs to two degenerate δ-bonds with 0.1518 a.u. energy in α-part, and two different directions which are perpendicular to each other ($d_{xy}^{100.0}$-$d_{xy}^{100.0}$ and d_{x2-y2}^{100}-d_{x2-y2}^{100}). The idealized natural Lewis-like structure is found to be quite high as 99.89 and 99.88% in α- and β-spin parts, respectively, indicating that a majority of electrons are localized. High localization of this system is further supported by the complete occupancy of NBOs where no significant charge transfer is observed between orbitals.

V_3 Cluster. Different initial geometries of trimmer, linear, bent, and isosceles triangle structures, were optimized for different multiplicities (2, 4, 6 and 8). Isosceles triangle (C_{2v}) of V_3 is in real minimum, while linear and bent structures show imaginary frequencies. Results of our calculations, including geometrical

Table 1. Bond length, d, (Å), Vibrational Frequency, ωe, (cm⁻¹), Bond Dissociation Energy, BDE, (eV), and Adiabatic Ionization Potential, IP_{ad}, (eV), Employed for Triplet V_2 Cluster

Method	Basis set	d (Å)	ωe (cm⁻¹)	BDE (eV)	IP_{ad} (eV)	Ref.
EXP.	-	1.774[a]	535.1[a]	2.753[b]	6.350[b,c]	[45][a]
mPWPW91	**QZVP**	**1.774**	**634.6**	**2.742**	**6.643**	-
BP86	QZVP	1.773	637.4	4.265	6.789	[4][b]
BPW91	QZVP	1.775	634	2.537	6.599	[46][c]
M05	DGDZVP2	1.778	658.4	1.904	6.572	
TPSS	QZVP	1.777	641.7	2.581	6.412	
TPSS	TZVP	1.764	658.2	3.041	6.215	
BPL	6-311+G*	1.761	625.6	3.181	6.947	
TPSSh	QZVP	1.758	665.5	1.384	6.205	
B3LYP	QZVP	1.670	767.8	0.468	6.102	
BLYP	QZVP	1.786	622.6	3.254	6.611	
BPL	QZVP	1.791	614.4	2.954	6.948	

Table 2. Calculated Bond Dissociation Energy, BDE, (eV), Adiabatic Ionization Potential, IP_{ad} (eV) for V_n (n = 3-5) at mPWPW91/ QZVP Level of Theory
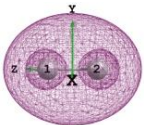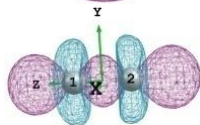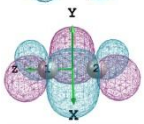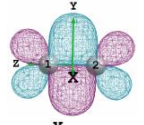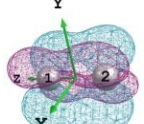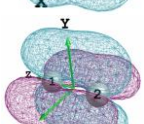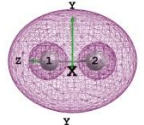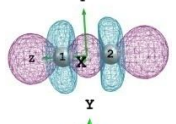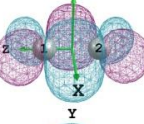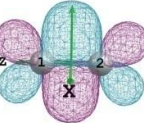
V_n	BDE	EXP.[a]	IP_{ad}	EXP.[a]	Ref.
3	2.04	1.42 ± 0.1	6.16	5.49 ± 0.05	[4][a]
4	2.93	3.67 ± 0.11	4.93	5.63 ± 0.05	
5	3.02	3.08 ± 0.18	4.83	5.47 ± 0.05	

parameters and energy information (BDE, IP_{ad} and EA), are shown in Table 4. These results show that there are two equal long bonds, 2.203 Å, a short bond, 1.864 Å, and apex angle, 50.0°, in doublet spin state with BDE and IP_{ad} of 2.04 eV and 6.16 eV. These results are close to other reports [4,17-19], as shown in Table 4.

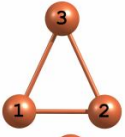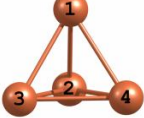The results of NBO calculations are collected in Table

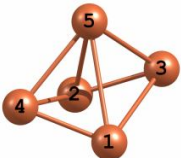1s. The largest multiplicity of the bonds is observed in β-set for $V_{(1)}$-$V_{(2)}$ which is quadruple, and other bonds are single or double in character in either spin-set. NBO shows that total Lewis electron densities for α- and β-spin parts are 97.17 and 96.71%, respectively. This reduction in Lewis density caused by depletion of occupancies of molecular orbitals means that there are delocalization, significant total

Table 3. NBOs, Orbital Hybridization in Percentage, Energy, and Shape of NBOs in Triplet V_2 Cluster

NBO bonds	h_A-h_B (%)	Energy (a.u.)	NBO picture
α-spin part			
$\sigma_{V(1)-V(2)}$	$s^{99.4}$-$s^{99.4}$	-0.3345	
$\sigma_{V(1)-V(2)}$	$d_{z^2}^{100.0}$ - $d_{z^2}^{100.0}$	-0.1962	
$\pi_{V(1)-V(2)}$	$d_{xz}^{98.4}$-$d_{xz}^{98.4}$	-0.1958	
$\pi_{V(1)-V(2)}$	$d_{yz}^{98.4}$-$d_{yz}^{98.4}$	-0.1958	
$\delta_{V(1)-V(2)}$	$d_{xy}^{100.0}$-$d_{xy}^{100.0}$	-0.1518	
$\delta_{V(1)-V(2)}$	d_{x2-y2}^{100}-d_{x2-y2}^{100}	-0.1518	
β-spin part			
$\sigma_{V(1)-V(2)}$	$s^{99.4}$-$s^{99.4}$	-0.3349	
$\sigma_{V(1)-V(2)}$	$d_{z^2}^{100.0}$ - $d_{z^2}^{100.0}$	-0.1762	
$\pi_{V(1)-V(2)}$	$d_{xz}^{98.4}$-$d_{xz}^{98.4}$	-0.1782	
$\pi_{V(1)-V(2)}$	$d_{yz}^{98.4}$-$d_{yz}^{98.4}$	-0.1782	
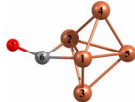
[*]Occupancy of all bonds is one.

Table 4. Calculated Parameters of Equilibrium Geometry (Bond Length, d, in Å and Angle in Degree), the BDE, (eV), the IP_{ad} (eV), and Relative Energy (ΔE) (kcal mol^{-1}) of Trimer to Pentamer

Optimized structure	Mul	ΔE	d_{V1-V2} / d_{V1-V4}	d_{V2-V3} / d_{V3-V4}	d_{V1-V3} / d_{V1-V5}	BDE	IP_{ad}	EA	Ref.
(trimer triangle)	2[a,c]	0.00	1.864	2.203[a]	2.203	2.04	6.16	0.97	[18][a]
Distorted tetrahedron	1[b,c]	0.00	2.259[b]	-	-	2.93	4.93	1.27	[19][b]
Rectangle	1[a,c]	3.6	1.757[c]	2.422	-	-	-	-	This work[c]
Rhombus	1[b,c]	1.3	2.091[c]	2.340	2.303	-	-	-	[4][d]
Distorted trigonal bi-pyramid	1[a,c]	0.0	2.541 / 2.453	2.410 / -	2.453 / 2.410	3.02 / (3.08)[d]	4.83 / (5.47)[d]	1.25 / (1.22)[e]	[17][e]
Non-planar square pyramid	1[c]	10.9	- / 2.500	2.500 / -	1.954 / 1.954	-	-	-	-

[a]Apex angle of trimer (∠V_1-V_3-V_2) is 50.0°. [b]All bonds of distorted tetrahedron have the same bond length. [c]Rectangle and rhombus have two short bonds and two long bonds.

Table 5. Gibbs Free Energy, Binding (Adsorption) Energy, and Interaction Energy (kcal mol^{-1}) and Bond Length, d, (Å) of the most Stable V_n-CO ($n = 2$-5) Complexes

CO	Structure	2S+1	ΔG	ΔE_{metal}	ΔE_{ligand}	E_{bind}	E_{int}	d_{C-O}	$d_{V(1)-C}$	$d_{V(2)-C}$ [a]
V_2 (Top)		3	-26.1	0.9	2.8	-26.1	-29.8	1.213	2.397	1.929
V_3 (Top)		2	-39.9	4.4	7.4	-50.9	-62.8	1.247	1.902	2.215
V_4 (Hollow)		1	-53.0	0.0	9.2	-49.2	-58.4	1.317	1.877	2.026
V_5 (Equatorial)		2	-74.2	7.2	29.1	-74.2	-110.5	1.358	1.925	2.009

[a]The number of vanadium atom in trimer and tetramer is 3.

Table 6. Interaction of the most Stable V_n ($n = 2$-5) Clusters with Oxygen Molecule, Gibbs Free Energy, Binding (Adsorption) Energy, and Interaction Energy (kcal mol^{-1}) and Bond Length, d, (Å)
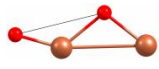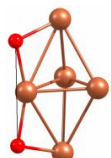
O_2	Structure	2S+1	ΔG	ΔE_{metal}	ΔE_{ligand}	E_{bind}	E_{int}	d_{O-O}
V_2 (Bridge)		5	-164.2	86.7	154.2	-163.9	-404.7	3.103
V_3 (Top)		4	-209.5	9.4	153.6	-214.0	-377.0	3.278
V_4 (Hollow)		3	-216.6	2.5	150.6	-216.3	-369.4	2.891
V_5 (Equatorial)		8	-221.4	7.5	144.9	-232.6	-385.0	3.572

Table 7. Primary and Secondary Hyper-conjugations in the V_nO_2 (n = 2-5) Complexes

Complexes	Spin set	Primary	E_2	secondary	E_2
V_2O_2	α	-		$n_{O(3)} \rightarrow \sigma_{V(1)-V(2)}$	29.9
V_3O_2	β	$\sigma_{V(2)-V(3)} \rightarrow \pi^*_{V(1)-O(5)}$	11.7	$\sigma_{V(2)-V(3)} \rightarrow \sigma^*_{V(1)-O(4)}$	22.4
		-	-	$\sigma_{V(2)-V(3)} \rightarrow \sigma^*_{V(1)-O(5)}$	24.4
		-	-	$n_{O(5)} \rightarrow \sigma^*_{V(1)-V(2)}$	13.2
V_4O_2	α	$\pi_{V(1)-O(5)} \rightarrow \sigma^*_{V(2)-O(6)}$	5.5	-	-
		$\pi_{V(3)-O(60} \rightarrow \sigma^*_{V(2)-O(5)}$	5.5	-	-
	β	-	-	$\sigma_{V(1)-V(3)} \rightarrow \sigma^*_{V(2)-O(6)}$	3.9
		-	-	$\sigma_{V(1)-V(4)} \rightarrow \sigma^*_{V(2)-O(5)}$	3.5
		-	-	$\sigma_{V(1)-O(5)} \rightarrow \sigma^*_{V(2)-V(4)}$	3.2
		-	-	$\sigma_{V(2)-V(4)} \rightarrow \sigma^*_{V(1)-O(5)}$	3.5
		-	-	$\sigma_{V(3)-V(4)} \rightarrow \sigma^*_{V(2)-O(6)}$	3.8
V_5O_2	α	-	-	$n_{O(7)} \rightarrow \sigma^*_{V(1)-V(2)}$	7.9
		-	-	$n_{O(7)} \rightarrow \sigma^*_{V(1)-V(5)}$	8.4
	β	-	-	$n_{O(6)} \rightarrow \sigma^*_{V(1)-V(2)}$	4.8
		-	-	$n_{O(6)} \rightarrow \sigma^*_{V(1)-V(5)}$	4.8
		-	-	$n_{O(7)} \rightarrow \sigma^*_{V(1)-V(2)}$	4.8
		-	-	$n_{O(7)} \rightarrow \sigma^*_{V(1)-V(5)}$	4.8

donor acceptor interaction 264.1 kcal mol^{-1} (see Table 2s).

Alternative structures for the reference NBO structure are expressed in the language of natural resonance theory (NRT) [48-50]. The NRT, implemented in the program package GenNBO [51] in which adding the resonance and reference structures [52] is a correction for the single NBO description. Four and three reference structures were introduced for highly delocalized V_3 cluster, as shown in Fig. 1. Many structures with very low percentages are not shown in this figure. As judged by weightings of NRT, in α-part, the percentages of resonance structures are 22.9, 20.90, 18.18 and 12.74, and for β-spin part, the corresponding values are 35.75, 17.60 and 17.60, respectively

V_4 Cluster. Three initial geometries, tetrahedron,

rhombus, and rectangle, have been considered for V_4 cluster. A series of possible spin multiplicities (1, 3 and 5) were examined for all initial structures of these clusters. Contrary to some reports [18,19], our results show that the singlet distorted tetrahedron with C_1 symmetry and positive frequency is very close to regular tetrahedral which is the most preferred structures for V_4 cluster. Thus, the results suggest that equilibrium geometry of this structure has the same bond length equal to 2.259 Å, and different bond angles 59.9º and 60.1º. BDE and IP_{ad} of V_4 cluster are 2.93 eV and 4.93 eV, respectively. The other isomers of V_4, rhombus and rectangle, are found to be 1.3 and 3.6 kcal/mol higher than ground state, respectively, see Table 4.

The NBO descriptors of the singlet ground state

α set
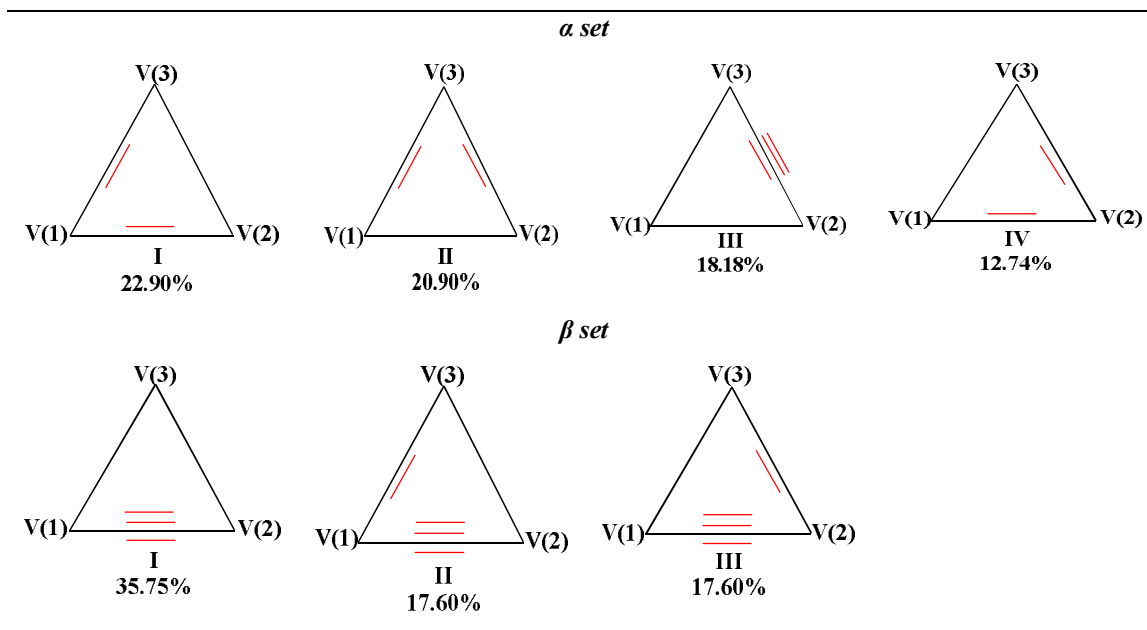
Fig. 1. The quantitative NRT resonance weightings for reference structures in the equilibrium V_3 geometry on two spin sets.
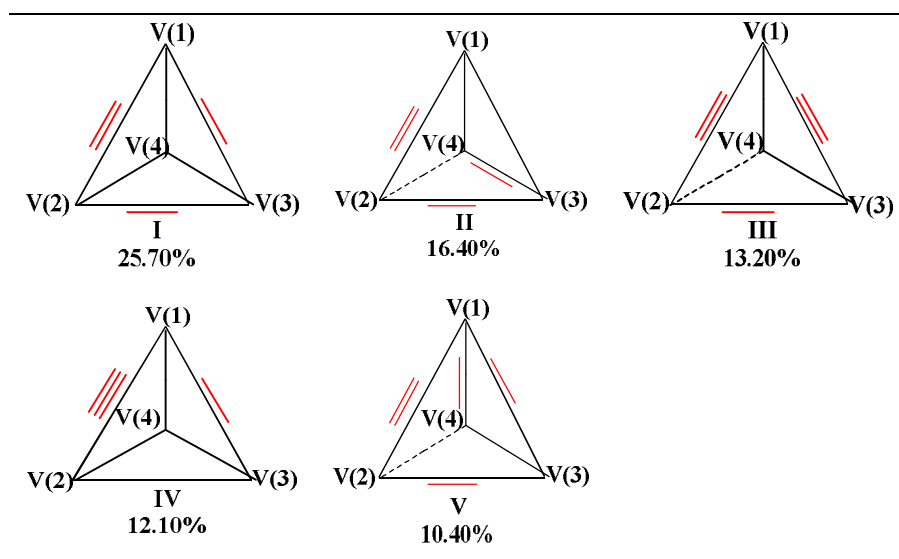
Fig. 2. The NRT descriptions of V_4 cluster for different reference structures.

structure show six degenerate σ bond orbitals and four degenerate three center/two electron (3C/2e) bonds for tetramer cluster, as shown in Table 3s, and they have a little depletion in occupancies. The four 3C/2e bonds are HOMOs with the same occupancy (1.946) and the same energy, -4.98 eV. The localized Lewis-like description of

density was found to be reasonably high (98.92%), which are relative good localized. All orbitals have significant depletion in occupancies and therefore cause twelve equal donor acceptor interactions from σ-bonds to the NB[*] orbitals of vanadium atoms with total energy of 248.4 kcal/mol. These are indication of existing resonance structures. The NRT descriptions with significant weight percentage of structures (25.70, 16.40, 13.20, 12.10 and 10.40) are also shown in Fig. 2.

V$_5$ Cluster. Our calculations started with two structures in pentamer cluster, distorted trigonal bi-pyramid (DTBP) and non-planar square pyramid (NPSP), with possible multiplicities 2, 4 and 6. The equilibrium geometry, energy properties (BDE, IP$_{ad}$ and EA) and spin multiplicity of these clusters are shown in Table 4. Doublet DTBP structure was optimized as ground state with C$_1$ symmetry, and NPSP structure lies 10.9 kcal mol^{-1} above the DTBP structure.

NBO-based analysis shows that this cluster has only two center/two electron (2C/2e) bonds, as shown in Table 4s. Almost all bonding and NB orbitals have considerable depletion in occupancies, specially NB orbitals in α-set and π$_{V(1)-V(2)}$ bond in β-set, which means that they have a considerable reactivity. In spite of the fact that the HOMO is NB orbitals of V(1) atom in α-set.

Total Lewis of 96.8 and 95.3% in α and β-spin parts, respectively, and significant depletion of occupancy in bonding orbitals which leads to the significant donor acceptor interactions (totally 494.1 kcal mol^{-1}), shown in Table 5s, are indication of a high delocalization in the target system. All these values show that vanadium pentamer has some resonance structures. The NRT calculation gives 1172 resonance structures with very small contributions.

Interaction of the V$_n$ (n = 2-5) Clusters with Small Ligands

CO adsorption on the V$_n$ (n = 2-5) clusters. In this part, possible adsorption modes of CO on the pure vanadium clusters (Fig. 3) are investigated. All of the possible spin multiplicities for complexes are examined. Our calculation reveals that spin multiplicity of the ground state complexes is the same as the pure clusters. The orientation of the ligand is a determining factor in probability of adsorption and the energy of interaction. The most stable vanadium adsorption structures are shown in

Table 5.

One way to recognize the catalytic activity is determination of the bond length and vibrational frequencies of small molecules adsorbed on the metal clusters. The elongation of the C-O bond length confirms the adsorption of CO on the vanadium clusters. In optimized complexes, the elongations of the C-O bond length are about 0.085, 0.119, 0.189 and 0.230 Å in V$_n$CO (n = 2-5) complexes, respectively. Stretching mode of C-O depends on the size of vanadium clusters; *i.e.*, it decreases significantly with the cluster size and causes the red shift. The vibrational frequency of the free CO molecule is 1976 cm^{-1}, whereas it decreases to 1673, 1664, 1566 and 1410 cm^{-1} for V$_n$CO (n = 2-5) complexes, respectively. The amount of red shift of C-O, shown in Fig. 4, also reflects the strength of the CO adsorption. This phenomenon can be explained by donation and back donation from NBO results, which all have stronger donation than back donation, see Table 6s.

The more negative values of the E$_{int}$ in the optimized structures indicate that the adsorptions are favorable and these sites are more active for interaction, as shown in Table 5. Figure 5 shows decreasing of E$_{int}$ as a function of the size from V$_2$ to V$_5$ clusters. According to this figure, the significant E$_{int}$ belongs to the V$_5$CO structure.

The Lewis-like description of V$_n$CO (n = 2-5) bonding is illustrated by the NBO analysis, see Table 7s. The V$_n$ (n = 2-5) clusters with partially filled orbitals act as donor in the interactions, while the CO molecule with special geometry acts as an acceptor ligand. The shifts of energies in vanadium clusters and CO lead to overall stabilization of complexes and π-back bonding of the CO ligand.

O$_2$ Adsorption on V$_2$ to V$_5$ clusters. Interaction of vanadium cluster with oxygen molecule (triplet) is dissociative. Vanadium metal is oxidized very well. In a wide industrial application, vanadium oxide clusters can be employed as catalysis for the chemical processes [53]. In this section, geometry, electronic structure, and bonding character of V$_n$O$_2$ (n = 2-5) complexes will be presented.

The V$_n$O$_2$ (n = 2-5) complexes were optimized at different possible orientations, as shown in Fig. 3. According to Table 6, orientation of O$_2$ molecule is suitable at bridge, top, hollow, and equatorial sites in V$_2$ to V$_5$ clusters, respectively. The most stable configuration was found based on the lowest energy value. Remarkable energy
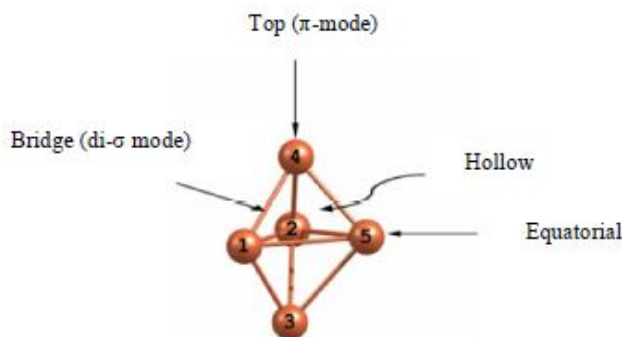
Fig. 3. Possible adsorption sites as initial geometries of ligand on vanadium clusters.
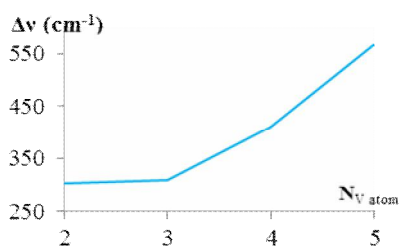

Fig. 4. The amount of red shift of carbon monoxide *vs*. number of vanadium atoms in the V_nCO (n = 2-5) complexes.
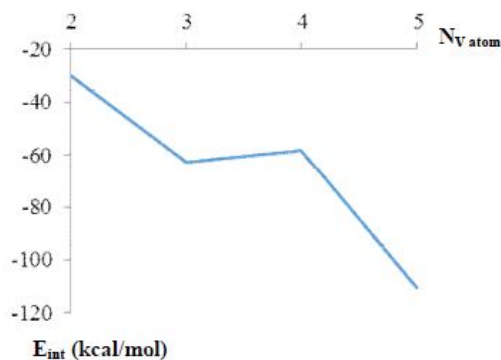
Fig. 5. The E_{int} values as a function of number vanadium atoms in the V_nCO (n = 2-5) complexes.

values of vanadium-oxygen complexes are due to the high deformation energies of the fragments. In general, restructuring of TM clusters over ligation is quite trivial except for V_2 cluster. Deformation energy of oxygen molecule is noticeably high that indicate they have appreciably changed over adsorption. In dissociative adsorption, oxygen atoms in the O_2 molecule are separated to large distance, as shown in Table 6. The V-O stretching frequency is higher for adsorption on stable mode with respect to other modes, indicating a stronger bond in these complexes. This supports the idea that oxygen is dissociatively adsorbed on vanadium clusters. The dissociative adsorption of the O_2 molecule on the TM clusters is very important for heterogeneous catalysis, material processing, and the epoxidation of ethylene [42,43].

The σ-bond framework explains 6.6-100% of *d*-orbital character in hybridization in the V_nO_2 (*n* = 2-5) complexes. Because of high electronegativity of oxygen we expect greater *d*-orbital character in the V-O metal hybrid. The valence of oxygen is varying from one to four when combined with *d*-orbital-block elements, as shown in Table 8s.

To show contribution of appreciable resonance stabilizations, hyper-conjugation concept is used. [54,55] The hyper-conjugation is the interaction of the electrons in the σ and π bond or NB orbitals with an adjacent empty NB, σ, and π anti-bonding orbitals. The primary and secondary hyper-conjugation [52] are σ→π* or π→σ* and σ→σ* or n→σ* interactions, respectively. Primary and secondary hyper-conjugation in these complexes are summarized in Table 7. As seen in this table, hyper-conjugation interactions are considerably strong in V_2O_2 and V_3O_2 (11-30 kcal mol^{-1}), whereas in V_4O_2 and V_5O_2 are weak (3-8 kcal/mol). These interactions in the V_nO_2 (*n* = 2-5) complexes typically polarize the V-O bonds, since these bonds have 6.6-23.8% metal character.

Donor acceptor interactions in the V_3O_2 and V_4O_2 complexes lead to depletion of occupancy of the occupied orbitals, and increasing occupancy of the unoccupied orbitals. Consequently, the bonds in these complexes are weakened. Significant charge transfers are $\pi_{V(2)-O(6)} \rightarrow n^*_{V(3)}$ and $\sigma_{V(1)-O(5)} \rightarrow n^*_{V(2)}$ in the V_4O_2 and V_3O_2 complexes, vs. $\pi_{V(1)-O(3)} \rightarrow n^*_{V(2)}$ in the V_2O_2 with associated second-order delocalization energies 13.0 and 60.3 kcal mol^{-1}. *vs.* 10.9, respectively. Therefore, strength of the V-O bonds in V_2O_2 is more than that of the V_3O_2 and V_5O_2 complexes.

CONCLUSIONS

We theoretically evaluated geometric and electronic structures of V_n (*n* = 2-5) clusters and V_nL complexes (L: CO and triplet O_2). The results show that vanadium clusters with number of even vanadium atoms have odd spin multiplicity, whereas those with number of odd vanadium atoms have even spin multiplicity. We also studied nature of chemical bonding of clusters and complexes by natural bond orbital (NBO) methodology. Natural resonance theory (NRT) method was also used to introduce resonance structures in pure trimer to pentamer vanadium clusters.

Interaction of ligands (triplet O_2 and CO) with pure vanadium clusters was considered. These interactions are associative with CO while are dissociative with oxygen molecule. Interaction energy in V_nO_2 complexes is greater than that of V_nCO complexes. Deformation energies of both vanadium clusters and CO ligand are very little in V_nCO complexes, while in triplet O_2 are high for ligand but very little for cluster, except for V_2 in V_nO_2 complexes.

Supporting Information

Supporting information (contains 8 Tables) is also available which includes significant charge transfers of pure vanadium clusters and NBO descriptions for complexes.

REFERENCES

[1] Linder, K., Die räumliche Konfiguration der Halogenderivate des zweiwertigen Molybdäns, Wolframs und Tantals. *Zeits Anorg. Allg. Chem.* **1927**, *162*, 203-221, DOI: 10.1002/zaac.19271620119.

[2] Cotton, F. A., Metal atom clusters in oxide systems, *Inorg. Chem.* **1964**, *3*, 1217-1220, DOI: 10.1021/ic50019a003.

[3] Klotzbucher, W. E.; Mitchell, S. A.; Ozin, G. A., Metal atom-metal cluster chemistry, *Inorg. Chem.* **1977**, *16*, 3063-3070, DOI: 10.1021/ic50178a017.

[4] Su, C.–X.; Hales, D. A.; Armentrout, P. B., Collision-induced dissociation of V*n*+ (*n* = 2-20) with Xe: Bond energies, dissociation pathways, and structures, *J. Chem. Phys.* **1993**, *99*, 6613-6623, DOI: 10.1063/1.465853.

[5] Sanpo, N.; Wen, C.; Berndt, C. C.; Wang, J., Antibacterial properties of spinel ferrite nanoparticles, E-Publishing Inc. Spain, 2013, pp. 239-250, DOI: 10.1016/j.actbio.2012.10.037.

[6] Lampropoulos, C.; Cain, J. M., Transition Metal Clusters: A Unique STEM Playground, *Austin. J. Nanomed. Nanotechnol.* 2014, ISSN: 2381-8956.

[7] Ozin, G. A.; Andrews, M. P., Arene-metal dimer complexes, bis(benzene) vanadium [$(C_6H_6)_2V_2$] and benzenevanadium [$(C_6H_6)V_2$]; experiment and

x.alpha. theory. 3, *J. Phys. Chem.* **1986**, *90*, 1245-1256, DOI: 10.1021/j100398a010.

[8] Ashley, A. E.; Cooper, R. T.; Wildgoose, G. G.; Green, J. C.; O'Hare, D., Homoleptic permethylpentalene complexes: "Double Metallocenes" of the first-row transition metals. *J. Am. Chem. Soc.* **2008**, *130*, 15662-15677, DOI: 10.1021/ja8057138.

[9] Ataf, A. A.; Hafeez, H.; Sumbal, A.; Nayab, S.; Amin, B., Medicinal importance of some metal cluster compounds, *J. Drug Design Med. Chem.* **2016**, *2*, 1-9, DOI: 10.11648/j.jddmc.20160201.11.

[10] Dorcier, A.; Ang, W. H.; Bolan˜o, S.; Gonsalvi, L.; Juillerat-Jeannerat, L.; Laurenczy, G.; Peruzzini, M.; Phillips, A. D.; Zanobini, F.; Dyson, P. J., *In Vitro* Evaluation of rhodium and osmium RAPTA analogues: The case for organometallic anticancer drugs not based on ruthenium. *Organometallics.* **2006**, *25*, 4090-4096, DOI: 10.1021/om060394o.

[11] Therrien, B.; Ang, W. H.; Che´rioux, F.; Vieille-Petit, L.; Juillerat-Jeanneret, L.; Su¨ss-Fink, G.; Dyson, P. J., Remarkable anticancer activity of triruthenium-arene clusters compared to tetraruthenium-arene clusters, *J. Cluster Sci.* **2007**, *18*, 741-752, DOI: 10.1007/s10876-007-0140-y.

[12] Simon, M. P.; Boss, S. R.; Paul, D. B., Tuning heavy metal compounds for anti-tumor activity is diversity the key to rutheniumrs success. *Future Med. Chem.* **2009**, *1*, 541-559, DOI: 10.4155/fmc.09.25.

[13] Nilekar, A.; Mavrikakis, J.; Manos, A., Simple rule of thumb for diffusion on transition-metal surfaces. *Angew. Chem. Int. Edit.* **2006**, *45*, 1521-3773, DOI: 10.1002/ange.200602223.

[14] Kanazawa, E.; Sakai, G.; Shimanoe, K.; Kanmura, Y., Teraoka, Y.; Miura, N.; Yamazoe, N., Metal oxide semiconductor N_2O sensor for medical use. *Sensors and Actuators B: Chem.* **2001**, *7*, 72-77, DOI: 10.1016/S0925-4005(01)00675-X.

[15] Freund, H. -J., Clusters and islands on oxides: from catalysis *via* electronics and magnetism to optics. *Surf. Sci.* **2002**, *500*, 271-299, DOI: 10.1016/S0039-6028(01)01543-6.

[16] Astruc, D., Organometallic Chemistry and Catalysis. Berlin. 2007, pp. 23-46, ISBN: 978-3-540-46129-6.

[17] Wu, H.; Desaei, S. R.; Wang, L. -S., Evolution of the electronic structure of small vanadium clusters from molecular to bulklike. *Phys. Rev. Lett.* **1996**, *77*, 2436-2439, DOI: 10.1103/PhysRevLett.77.2436.

[18] Grönbeck, H.; Rosen, A., Geometric and electronic properties of small vanadium clusters: A density functional study. *J. Chem. Phys.* **1997**, *107*, 10620-10625, DOI: 10.1063/1.474177.

[19] Wu, X.; Ray, A. K.; A density functional study of small neutral and cationic vanadium clusters Vn and $V_n+(n = 2\text{-}9)$. *J. Chem. Phys.* **1999**, *110*, 2437-2445, DOI: 10.1063/1.477949.

[20] Ratsch, C.; Fielicke, A.; Kiriliyuk, A.; Behler, J., von Helden, G.; Meijer, G.; Scheffler, M., Structure determination of small vanadium clusters by density functional theoryin comparison with experimental far-infrared spectr. *J. Chem phys.* **2005**, *122*, 124302-1-124302-15,DOI: 10.1063/1.1862621.

[21] Ghosh, P.; Raghani, P.; de Gironcoli, S.; Narasimhan, Sh., Interplay between bonding and magnetism in the binding of NO to Rh clusters. *J. Chem. Phys.* **2008**, *128*, 194708-1-194708-8, DOI: 10.1063/1.2913242.

[22] Holmgren, L.; Rosén, A., Vanadium clusters: Reactivity with CO, NO, O_2, D_2, and N_2. *J. Chem. Phys.* **1999**, *110*, 2629-2636, DOI: 10.1063/1.477984.

[23] Feyel, S.; Schroder, D.; Schwarz, H., Pronounced cluster-size effects: Gas-phase reactivity of bare vanadium cluster cations V*n*+ (*n* = 1-7) Toward Methanol. *J. Phys. Chem A.* **2009**, *113*, 5625-5632, DOI: 10.1021/jp901565r.

[24] Wu, G.; Yang, M.; Guo, X.; Wang, J., Comparative DFT study of N_2 and no adsorption on vanadium clusters V*n* (*n* = 2-13). *J. Comput. Chem.* **2012**, *33*, 1854-1861, DOI: 10.1002/jcc.23017.

[25] Swart, I.; Fielicke, A.; Redlich, B.; Meijer, G.; Weckhuysen, B. M.; de Groot, F. M., Hydrogen-induced transition from dissociative to molecular chemisorption of CO on vanadium clusters. *J. Am.*

Chem. Soc. **2007**, *31*, 2516-2520, DOI: 10.1021/ja066261b.

[26] Zeinalipour, Y.; Constantinos, D. C.; Andrew, L.; Efstathiou, A. M., CO adsorption on transition metal clusters: Trends from density functional theory. *Surf. Sci.* **2008**, *602*, 1858-1862, DOI: 10.1016/j.susc.2008.03.024.

[27] Weckhuysen, B. M.; Keller, D. E., Spectroscopy and role of supported vanadium oxides in hetrogeneous catalysis chemistry, *Catal. Today.* **2003**, *78*, 25-46, DOI: 10.1016/S0920-5861(02)00323-1.

[28] Lapina, O. B.; Bal'zhinimaev, B.; Boghosian, S.; Eriksen, K. M.; Fehrmann, R., Progress on the mechanistic understanding of SO$_2$ oxidation catalysts, *Catal. Today.* **1999**, *51*, 469-479, DOI: 10.1016/S0920-5861(99)00034-6.

[29] Taylor, K. C., Nitric oxide catalysis in automotive exhaust systems. *Catal. Rev.* **1993**, *35*, 457-481, DOI: 10.1080/01614949308013915.

[30] Bond, G. C.; Tahir, S. F., Vanadium oxide monolayer catalysts Preparation, characterization and catalytic activity. *Applied Catal.* **1991**, *71*, 1-31, DOI: 10.1016/0166-9834(91)85002-D.

[31] Foster, J. P.; Weinhold, F., Natural hybrid orbitals, *J. Am. Chem. Soc.* **1980**, *102*, 7211-7218, DOI: 10.1021/ja00544a007.

[32] Reed, A. E.; Weinstock, R. B.; Weinhold, F., Natural population analysis, *J. Chem. Phys.* **1985**, *83*, 735-746, DOI: 10.1063/1.449486.

[33] Frisch, M. J., Gaussian 09 revision A. 1. Wallingford, CT, USA, Gaussian, Inc., 2009.

[34] Furche, F.; Perdew, J. P., The performance of semilocal and hybrid density functionals in 3d transition-metal chemistry, *J. Chem. Phys.* **2006**, *124*, 044103-1-044103-27, DOI: 10.1063/1.2162161.

[35] Zhao, Y.; Truhlar, D. G., Comparative assessment of density functional methods for 3d transition-metal chemistry, *J. Chem. Phys.* **2006**, *124*, 2241051-2241056, DOI: 10.1063/1.2202732.

[36] Cramer, C. J.; Truhlar, D. G., Density functional theory for transition metals and transition metal

chemistry, *Phys. Chem. Chem. Phys.* **2009**, *11*, 10757-10816, DOI: 10.1039/B907148B.

[37] Cohen, A. J.; Mori-Sánchez, P.; Yang, W., Second-order perturbation theory with fractional charges and fractional spins. *J. Chem. Theor. Comput.* **2009**, *5*, 786-792, DOI: 10.1021/ct8005419.

[38] Perdew, J. P.; Burke, K.; Ernzerhof, M., Accurate and simple analytic representation of the electron-gas correlation energy. *Phy. Rev. B.* **1992**, *45*, 13244-13249, DOI: 10.1103/PhysRevB.45.13244.

[39] Adamo, C.; Barone, V., Exchange functionals with improved long-range behavior and adiabatic connection methods without adjustable parameters: The mPW and mPW1PW models. *J. Chem. Phys.* **1998**, *108*, 664-675, DOI: 10.1063/1.475428.

[40] Perdew, J. P.; Burke, K.; Ernzerhof, M., Generalized gradient approximation made simple, *Phys. Rev. Lett.* **1996**, *77*, 3865-3868, DOI: 10.1103/PhysRevLett.77.3865.

[41] Weigend, F.; Furche, F.; Ahlrichs, R., Gaussian basis sets of quadruple zeta valence quality for atoms H-Kr. *J. Chem. Phys.* **2003**, *119*, 12753-12762, DOI: 10.1063/1.1627293.

[42] Groß, A.; Eichler, A.; Hafner, J.; Mehl, M. J.; Papaconstantopoulos, D. A., Unified picture of the molecular adsorption process: O$_2$/Pt(111). *Surf. Sci.* **2003**, *539*, L542-L548, DOI: 10.1016/S0039-6028(03)00791-X.

[43] Gao, W.; Zhao, M.; Jiang, Q., A DFT study on electronic structures and catalysis of Ag$_{12}$O$_6$/Ag(111) for ethylene epoxidation. *J. Phys. Chem. C.* **2007**, *111*, 4042-4046, DOI: 10.1021/jp0684729.

[44] Kang, G. J.; Chen, Z. X.; Li, Z., Theoretical studies of the interactions of ethylene and formaldehyde with gold clusters. *J. Chem. Phys.* **2009**, *131*, 034710-034718, DOI: 10.1063/1.3167408.

[45] Langridge-Smith, P. R. R.; Morse, M. D.; Hansen, G. P.; Smalley, R. E.; Merer, A. J., The bond length and electronic structure of V$_2$. *J. Chem. Phys.* **1984**, *80*, 593-600, DOI: 10.1063/1.446769.

[46] Kant, A.; Lin. S. S., Dissociation Energies of Ti$_2$ and

V_2. *J. Chem. Phys.* **1969**, *51*, 1644-1647, DOI: 10.1063/1.1672226.

[47] Walch, S. P.; Bauschlicher Jr, C. W.; Roos, B. O.; Nelin, C. J., Theoretical evidence for multiple 3d bondig in the V2 and Cr2 molecules. *Chem. Phys. Lett.* **1983**, *103*, 175-179, DOI: 10.1016/0009-2614(83)80376-5.

[48] Glendening, E. D.; Weinhold, F., Natural resonance theory I, *J. Comput. Chem.* **1998**, *19*, 593-609, DOI: 10.1002/(SICI)1096-987X(19980430)19:6<593::AID-JCC3>3.0.CO;2-M.

[49] Glendening, E. D.; Weinhold, F., Natural resonance theory: II. *J. Comput. Chem.* **1998**, *19*, 610-627, DOI: 10.1002/(SICI)1096-987X(19980430)19:6<610::AID-JCC4>3.0.CO;2-U.

[50] Glendening, E. D.; Weinhold, F., Natural resonance theory: III, *J. Comput. Chem.* **1998**, *19*, 628- 646, DOI: 10.1002/(SICI)1096-987X(19980430)19:6<628: AID-JCC5>3.0.CO;2-T.

[51] Glendening, E. D.; Badenhoop, J. K.; Reed, A. E.; Carpenter, J. E.; Bohmann, J. A.; Morales, C. M.; Weinhold, F., GenNBO 5.0. Theoretical Chemistry Institute, University of Wisconsin, Madison, WI, 2001.

[52] Weinhold, F.; Landis, C., Valancy and Bonding. Wisconsin 2005, Chapter 3-5, ISBN 13: 978-0-511-11548-6.

[53] Fierro, J. L. G.; Raton, B., Metal Oxidees Chemistry and Applications., Talor-Franceis. 2005, Chapter 1, ISBN: 9780824723712 - CAT# DK3029.

[54] Mulliken, R. S., Intensities of electronic transitions in molecular spectra IV. Cyclic dienes and hyperconjugation. *J. Chem. Phys.* **1939**, *7*, 339-352, DOI: 10.1063/1.1750446.

[55] Mulliken, R. S.; Rieke, C. A.; Brown, W. G., Hyperconjugation. *J. Am. Chem. Soc.* **1941**, *63*, 41-56, DOI: 10.1021/ja01846a008.